

## Charge Transfer in Photoacids Observed by Stark Spectroscopy

Lisa N. Silverman, D. B. Spry, Steven G. Boxer, and M. D. Fayer\*

Department of Chemistry, Stanford University, Stanford, California 94305

Received: June 12, 2008; Revised Manuscript Received: July 31, 2008

The charge redistribution upon photoexcitation is investigated for a series of pyrene photoacids to better understand the driving force behind excited-state proton-transfer processes. The changes in electric dipole for the lowest two electronic transitions ( ${}^1L_b$  and  ${}^1L_a$ ) are measured by Stark spectroscopy, and the magnitudes of charge transfer of the protonated and deprotonated states are compared. For neutral photoacids studied here, the results show that the amount of charge transfer depends more upon the electronic state that is excited than the protonation state. Transitions from the ground state to the  ${}^1L_b$  state result in a much smaller change in electric dipole than transitions to the  ${}^1L_a$  state. Conversely, for the cationic (ammonium) photoacid studied, photoexcitation of a particular electronic state results in much smaller charge transfer for the protonated state than for the deprotonated state.

### I. Introduction

Certain aromatic dyes undergo a profound change in  $pK_a$  upon photoexcitation. The subset of these dyes that have a lower  $pK_a$  in the excited state than in the ground state are known as photoacids. Photoacids have been studied extensively over the last half-century due to their myriad applications.<sup>1–3</sup> For example, proton-transfer processes are ubiquitous in chemistry and biology, and photoacids are useful in the investigation of the general mechanisms by which fast proton-transfer reactions occur.<sup>2</sup> Photoacids also provide an efficient means of generating protons at a specific time, and this concept has been used extensively in the development of polymers for photolithography.<sup>4–6</sup> The change in acidity between the ground and excited states of photoacids can be extraordinary, with the acidity equilibrium constant ( $K_a$ ) differing by more than 10 orders of magnitude in some cases.<sup>7</sup> Photoacids have been studied in both gas and condensed phases, with benzene and naphthalene derivatives examined most often in the gas phase,<sup>8–11</sup> and naphthalene and pyrene derivatives studied more extensively in condensed phases.<sup>12–17</sup> However, there are many other types of aromatic molecules that also display an excited-state shift in  $pK_a$ , including hydroxystilbenes,<sup>18</sup> triarylaminines,<sup>19</sup> and the chromophore of Green Fluorescent Protein (GFP).<sup>20,21</sup> The work presented below will focus specifically on the pyrene derivatives shown in Figure 1.

Despite the wealth of literature describing both experimental and theoretical studies of photoacids, the mechanism by which the  $pK_a$  is lowered in the excited state relative to the ground state is not clearly understood. It is generally agreed that a charge rearrangement occurs such that electron density is transferred from the acidic moiety, often a hydroxyl group, to the aromatic ring.<sup>3</sup> However, there is disagreement as to which protonation state undergoes the charge rearrangement and at what point in time such a rearrangement occurs.

In the first scenario, which is the more traditional view, the large change in acidity is attributed to an intramolecular charge transfer in the protonated state directly upon excitation. It is thought that upon photoexcitation, there is an  $n$  to  $\pi^*$  transition in which the nonbonding electrons on the hydroxyl oxygen are

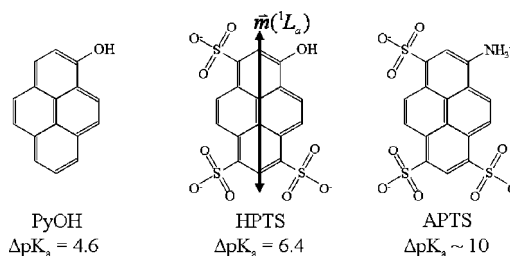


**Figure 1.** Pyrene photoacids probed by Stark spectroscopy and their  $\Delta pK_a$  values upon photoexcitation. The  ${}^1L_a$  transition dipole of all three molecules lies along the long molecular axis.

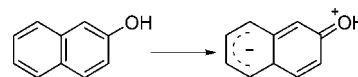


**Figure 2.** Model for charge redistribution in the excited state of protonated photoacids.

transferred into the  $\pi$  system of the photoacid.<sup>22</sup> This results in a partial positive charge on the oxygen and a partial negative charge on the aromatic ring, as shown in Figure 2. This partial positive charge on the oxygen reduces the proton affinity of the molecule, thereby shifting the acid–base equilibrium in the excited state by making the protonated form of the molecule a stronger acid than it is in the ground state. This explanation has been called into question by calculations showing that there is no significant  $n$  to  $\pi^*$  character in the lowest excited states of naphthalene and pyrene photoacids.<sup>23,24</sup>

A second scenario is that there is no significant charge rearrangement directly upon photoexcitation of the protonated state of the photoacid. Rather, the charge rearrangement occurs in the deprotonated state, such that the negative charge on the oxygen is delocalized into the aromatic ring, thereby making the excited anionic state less basic than the ground-state anion. The argument in this scenario is that photoacids become stronger acids in the excited state because the conjugate bases become weaker bases than they are in the ground state.<sup>23,25</sup> This notion that charge transfer happens primarily after proton transfer has occurred has been supported by recent gas-phase *ab initio* and semiempirical calculations.<sup>26,27</sup> However, there is some experimental evidence to the contrary. For example, ultrafast experi-

\* fayer@stanford.edu.

ments on the rates of dissociation and recombination of the photoacid 8-hydroxypyrene-1,3,6-trisulfonate (HPTS) show that the rate of dissociation in the excited state increases by about 5 orders of magnitude, from about  $10^5$  to  $10^{10}$  s<sup>-1</sup>, whereas the proton recombination rate in the conjugate photobase decreases by only 2 orders of magnitude, from less than  $10^{12}$  s<sup>-1</sup> to slightly greater than  $10^9$  s<sup>-1</sup>.<sup>15</sup> These data are more consistent with the first scenario, in which the change in  $pK_a$  is driven by a change in the acidity of the photoacid rather than by a change in the basicity of the photobase.

The models are not necessarily limited to one of the two extremes.<sup>3</sup> Both processes can coexist to shift the acid–base equilibrium from both sides of the proton-transfer reaction. The fundamental question regarding the mechanism for photoacidity is then reframed as, “Is charge transfer in the protonated photoacid or conjugate base more important for determining the  $pK_a$  shift, and what influences the relative strengths?”

Stark spectroscopy is a technique that is well suited to probing the validity of these two scenarios because it permits for the direct measurement of the change in charge distribution,  $\Delta\vec{\mu}$ , of a molecule between the ground and excited state of a particular electronic transition. By measuring the Stark effect for the visible absorption bands of photoacids in both the protonated and deprotonated states, it is possible to determine in which of these two states the charge redistribution occurs. It is worth noting that the Stark effects of the absorption bands can only provide information about charge-transfer processes that occur directly upon excitation, which would be problematic if the charge rearrangement occurred at some time after excitation. However, usually a simple Förster cycle calculation can be used to predict the  $pK_a$  accurately from the absorption spectra of the photoacid and conjugate base, assuming that the 0–0 energies can be found.<sup>28</sup> For example, the predicted  $\Delta pK_a$  values for pyrenol and HPTS, two of the photoacids used in this study, are 4.3 and 6.9, respectively, which is in excellent agreement with the experimental values of 4.6 and 6.4.<sup>29,30</sup> This validation of the Förster relation implies that, from a thermodynamics perspective, the mechanism responsible for photoacidity is reflected in the absorption spectrum.

## II. Materials and Methods

**A. Sample Preparation.** 1-Pyrenol (PyOH), 8-hydroxypyrene-1,3,6-trisulfonate (HPTS), and 8-aminopyrene-1,3,6-trisulfonate (APTS) were purchased from Fluka. In general, 1–2 mg of compound was dissolved in 20  $\mu$ L of 1:1 water/glycerol, which forms a glass at 77 K. None of the compounds used in this study are known to form dimers in the ground state, even at high concentrations. To generate the deprotonated forms of these molecules, 100 mM NaOH(aq) was substituted for the pure water in the solvent. Because APTS is only partially protonated at neutral pH, 100 mM HCl(aq) was substituted for the pure water in the solvent to generate the fully protonated form of this molecule. The optical densities of the samples were  $\sim 0.1$ . Sample solutions were loaded into the sample cell and immediately plunged into liquid nitrogen. The sample cell consisted of two unpolished float glass slides coated with indium tin oxide ( $R_s = 30\text{--}60$   $\Omega$ , Delta Technologies), separated by  $\sim 50$   $\mu$ m thick Kapton spacers, and mechanically held together with clips. Actual sample cell thicknesses were measured by recording the spectral interference fringes from 600 to 1100 nm produced by the inner surfaces of the sample cell windows. Frozen glass samples were used to ensure that there is an isotropic sample and that no poling occurs in response to the applied electric field.

**B. Stark Spectroscopy Apparatus.** Light from a mercury–xenon arc lamp was passed through a 0.22 m single monochromator, focused through the sample, and detected with a silicon photodiode. An AC field was supplied by a custom-built high-voltage power supply or a Trek Model 10/10 high voltage power supply, which amplified an externally supplied, digitally generated sinusoidal voltage. Low temperature spectra were taken in a liquid nitrogen immersion cryostat.<sup>31</sup> The Stark signal ( $\Delta I$ ) was recorded with a lock-in amplifier (Stanford Research Systems SRS830) detecting at the second harmonic of the applied external field. The direct output voltage of the silicon photodiode ( $I$ ) was recorded as well so that the change in absorption of the sample due to the externally applied field was calculated as  $\Delta A = (2\sqrt{2}/\ln 10) \cdot (\Delta I/I)$ . Absorption spectra were taken on the same setup as the Stark spectra and the largest peak of each spectrum was scaled to unity. Stark spectra have been scaled to an external electric field of 1 MV/cm.

**C. Analytical Model for Stark Spectra.** For many electronic transitions involving only two electronic states, Stark effects are expected to cause a small peak shift in the absorption spectrum for a molecule but no change in line shape. This shift can be described by a Taylor series truncated at second order in  $\vec{F}$  as follows:

$$\Delta\bar{\nu} = -\frac{1}{hc} \left( \Delta\vec{\mu} \cdot \vec{F} + \frac{1}{2} \vec{F} \cdot \Delta\alpha \cdot \vec{F} + \dots \right) \quad (1)$$

where  $\vec{F}$  is the applied electric field, and  $\Delta\vec{\mu}$  and  $\Delta\alpha$  are the difference dipole moment and the difference polarizability, respectively, between the ground and excited states. In addition, the electric field also affects the transition dipole moment,  $\vec{m}$ , of the transition as follows:

$$\vec{m}(\vec{F}) = \vec{m} + \mathbf{A} \cdot \vec{F} + \vec{F} \cdot \mathbf{B} \cdot \vec{F} + \dots \quad (2)$$

where  $\mathbf{A}$  and  $\mathbf{B}$  are the transition polarizability and transition hyperpolarizability, respectively.

When eqs 1 and 2 are combined and integrated over all orientations in an isotropic sample, the Stark spectrum can be expressed as a sum of the derivatives of the absorption spectrum

$$\Delta A(\bar{\nu}) = \vec{F}^2 \left\{ A_\chi A(\bar{\nu}) + \frac{B_\chi}{15hc} \bar{\nu} \frac{d}{d\bar{\nu}} \left( \frac{A(\bar{\nu})}{\bar{\nu}} \right) + \frac{C_\chi}{30h^2c^2} \bar{\nu} \frac{d^2}{d\bar{\nu}^2} \left( \frac{A(\bar{\nu})}{\bar{\nu}} \right) \right\} \quad (3)$$

where the zeroth, first, and second derivative coefficients  $A_\chi$ ,  $B_\chi$ , and  $C_\chi$ , respectively, are

$$A_\chi = \frac{1}{30|\vec{m}|^2} \sum_{ij} [10A_{ij}^2 + (3\cos^2\chi - 1)(3A_{it}A_{jj} + A_{ij}^2)] + \frac{1}{15|\vec{m}|^2} \sum [10\vec{m}_t B_{ij} + (3\cos^2\chi - 1)(4\vec{m}_t B_{ij})] \quad (4)$$

$$B_\chi = \frac{5}{2} \text{Tr}(\Delta\alpha) + (3\cos^2\chi - 1) \left( \frac{3}{2} \Delta\alpha_m - \frac{1}{2} \text{Tr}(\Delta\alpha) \right) + \frac{1}{\vec{m}^2} \sum_{ij} [10\vec{m}_t A_{ij} \Delta\vec{\mu}_j + (3\cos^2\chi - 1)(3\vec{m}_t A_{ij} \Delta\vec{\mu}_i + \vec{m}_t A_{ij} \Delta\mu_j)] \quad (5)$$

$$C_\chi = |\Delta\vec{\mu}|^2 \cdot [5 + (3\cos^2\chi - 1)(3\cos^2\zeta_A - 1)] \quad (6)$$

In these equations,  $\chi$  is the experimental angle between the externally applied field and the polarization of incident light,  $\zeta_A$  is the angle between  $\Delta\vec{\mu}$  and  $\vec{m}$ , and  $\Delta\alpha_m$  is the component of the polarizability change along the direction of the transition

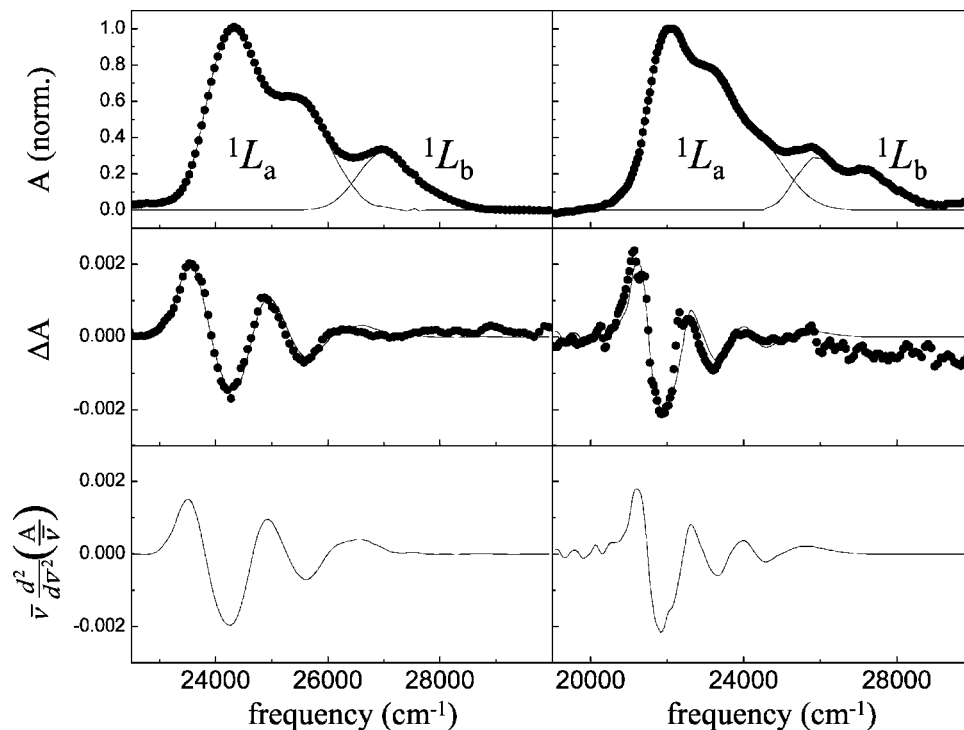


**Figure 3.** Absorption and Stark spectra of protonated (left) and deprotonated (right) HPTS. Top panels: absorption spectra (circles) and deconvolution of the spectra into  ${}^1L_a$  and  ${}^1L_b$  (solid lines) components. Middle panels: Stark spectra (circles) and fits of the Stark spectra to a sum of zeroth, first, and second derivatives of the absorption spectra (lines). Bottom panels: second derivative components of the fits to the  ${}^1L_a$  band. The second derivative of the  ${}^1L_b$  band is not included because it does not contribute to the Stark spectrum.

moment. The indices  $i$  and  $j$  are used for individual components of the vectors and tensors and run over the molecular coordinates  $x$ ,  $y$ , and  $z$ .

If  $\chi$  is set to  $54.7^\circ$ , then  $C_\chi$  depends only on  $\Delta\bar{\mu}$ . Therefore, the value of  $\Delta\bar{\mu}$  can be determined directly from the second derivative component of the Stark spectrum. The value of  $\zeta_A$  can also be determined from the second derivative component by illuminating the sample with horizontally polarized light, varying the angle  $\chi$  of the sample with respect to the light, and taking the ratio of the second derivative components of the resulting Stark spectra. If the Stark spectrum is dominated by the second derivative component,  $\zeta_A$  can be found by taking the ratio of the intact Stark spectra at various angles of  $\chi$ . The first derivative term has contributions from two different origins. The cross term between the transition polarizability,  $\mathbf{A}$ , and  $\Delta\bar{\mu}$  is generally small, particularly for small values of  $\Delta\bar{\mu}$ , and therefore it can be neglected. In addition, it is reasonable to assume that the main contribution to  $\Delta\alpha$  lies along the direction of the transition moment. With these assumptions, the first derivative contribution becomes linearly related to the change in polarizability, such that  $B_\chi = 5/2 \text{Tr}\Delta\alpha$  at  $\chi = 54.7^\circ$ . The zeroth derivative term has contributions from the transition polarizability,  $\mathbf{A}$ , and the transition hyperpolarizability,  $\mathbf{B}$ . In the cases studied here, the zeroth derivative makes a small but significant contribution to the Stark spectrum. Because the contributions from  $\mathbf{A}$  and  $\mathbf{B}$  cannot be distinguished from the experimental data, we report the raw fitting parameter,  $A_\chi$ .

All of the absorption spectra contain overlapping bands. For each spectrum the underlying bands were obtained by fitting the entire spectrum to a sum of Gaussians and making the energies consistent with the corresponding MCD spectrum, which clearly resolves the two states.<sup>32</sup> The MCD studies were conducted in the same solvent (glycerol) used in the Stark measurements, which allows for a direct comparison. In several cases, the overlapping absorption bands give rise to two

overlapping bands in the Stark spectrum, each of which has different fit electro-optic parameters. In these cases, the Stark spectrum of each absorption band was fit to a sum of derivatives in the nonoverlapping region of the spectrum. It was assumed that the coefficients of the derivative components are constant across any single absorption band. This assumption is confirmed in this study when only one absorption band is dominated by the Stark spectrum. Accordingly, in the overlap region, the sum of derivatives was generated for each band using the coefficients obtained in the nonoverlapping region, and the results for the two bands were added to obtain the total fit to the Stark spectrum. By this analysis, we assume that the electro-optic parameters obtained in the nonoverlapping region are the same in the overlapping region where direct measurement is not possible.

### III. Results and Discussion

**A. 8-Hydroxypyrene-1,3,6-trisulfonate (HPTS).** The absorption spectra of protonated and deprotonated HPTS are shown in the top panels of Figure 3. The lowest energy absorption band of HPTS in both the protonated and deprotonated forms is composed of two separate electronic transitions, which were previously identified by MCD spectroscopy.<sup>32</sup> In Platt notation,<sup>33</sup> which was created to describe the electronic energy levels in catacondensed hydrocarbons, the lowest energy transition ( $S_0$  to  $S_1$ ) is to the  ${}^1L_a$  state and the higher energy transition ( $S_0$  to  $S_2$ ) is to the  ${}^1L_b$  state. Formally, transitions to L states are forbidden and have low oscillator strength; however, this is only strictly true for molecules with very high symmetry. The subscript “a” denotes energy levels having the electron density on the atoms and the nodal points on the bonds connecting the atoms. The subscript “b” denotes energy levels having electron density on the bonds and the nodal points on the atoms. In practice, this means that the  ${}^1L_a$  and  ${}^1L_b$  states are generally orthogonal to one another, with the  ${}^1L_a$

TABLE 1: Spectroscopic Parameters and Results of Fitting of the Stark Spectra

compound	prot state <sup>a</sup>	S <sub>1</sub>	S <sub>2</sub>	A <sub>χ</sub> <sup>b</sup> (10 <sup>-20</sup> m <sup>2</sup> /V <sup>2</sup> )	S <sub>0</sub> - S <sub>1</sub> Δα <sup>c</sup> (Å <sup>3</sup> )	Δμ <sup>d</sup> (D)	A <sub>χ</sub> <sup>b</sup> (10 <sup>-20</sup> m <sup>2</sup> /V <sup>2</sup> )	S <sub>0</sub> - S <sub>2</sub> Δα <sup>c</sup> (Å <sup>3</sup> )	Δμ <sup>d</sup> (D)
HPTS	prot	<sup>1</sup> L <sub>a</sub>	<sup>1</sup> L <sub>b</sub>	4	6	4.2	<i>e</i>	<i>e</i>	<2.0 <sup>f</sup>
	deprot	<sup>1</sup> L <sub>a</sub>	<sup>1</sup> L <sub>b</sub>	1	3	5.2	<i>e</i>	<i>e</i>	<2.0 <sup>f</sup>
PyOH	prot	<sup>1</sup> L <sub>b</sub>	<sup>1</sup> L <sub>a</sub>	4	5	0.9	-1	3	2.0
	deprot	<sup>1</sup> L <sub>a</sub>	<sup>1</sup> L <sub>b</sub>	3	6	2.9	<i>e</i>	<i>e</i>	<2.5 <sup>f</sup>
APTS	prot	<sup>1</sup> L <sub>b</sub>	<sup>1</sup> L <sub>a</sub>	-9	3	0.6	-4	-8	2.1
	deprot	<sup>1</sup> L <sub>a</sub>	<sup>1</sup> L <sub>b</sub>	-1	2	5.3	<i>e</i>	<i>e</i>	<2.1 <sup>f</sup>

<sup>a</sup> Protonation state of the compound, either protonated (prot) or deprotonated (deprot). <sup>b</sup> For an experimental angle  $\chi = 90^\circ$ ; errors are on the order of 25–50%. <sup>c</sup> Errors are on the order of 25–50%. <sup>d</sup> Errors are on the order of 10–20%. <sup>e</sup> Values cannot be determined because there was no observable Stark signal from this band. <sup>f</sup> Precise value cannot be determined, so an upper bound for the value is given.

state aligned along the long axis of the  $\pi$  system and the <sup>1</sup>L<sub>b</sub> state aligned along the short axis, although these orientations are altered somewhat in the compounds studied here due to their lowered symmetry.<sup>32</sup>

The Stark spectra,  $\Delta A$ , for the protonated and deprotonated forms of HPTS are shown in the middle panels of Figure 3. The second derivative components of the fits to the Stark spectra are shown in the bottom panels. The Stark spectra of HPTS closely match the second derivatives of the <sup>1</sup>L<sub>a</sub> lineshapes, demonstrating that a change in dipole moment exclusively from the <sup>1</sup>L<sub>a</sub> transition dominates the Stark effect in both protonation states. This result is consistent with solvatochromic studies of naphthalene-based photoacids, which indicate that the <sup>1</sup>L<sub>a</sub> state has more charge-transfer character than the <sup>1</sup>L<sub>b</sub> state.<sup>3</sup>

The magnitudes of the difference dipole moments,  $|\Delta\bar{\mu}|$ , obtained from the Stark spectra are summarized in Table 1. The value of  $\Delta\bar{\mu}$  between the ground and first excited states (<sup>1</sup>L<sub>a</sub>) for the protonated form of HPTS is 4.2 D, whereas for the deprotonated form it is 5.2 D. For comparison, one electron transferred from the hydroxyl oxygen to the center of the pyrene ring (about 3.5 Å) would correspond to  $\sim 16$  D. The values of  $\Delta\bar{\mu}$  measured for HPTS are in the typical range for what has been reported for common Coumarin dyes.<sup>34</sup> The influence of  $\Delta\bar{\mu}$  for the <sup>1</sup>L<sub>b</sub> transition on the Stark spectrum is much smaller in both protonation states. The contribution to the data depends on the second derivative of the absorption spectrum. Because the absorption is weaker and the line shape is featureless, the second derivative is small and the precise value of  $\Delta\bar{\mu}$  for the <sup>1</sup>L<sub>b</sub> transition cannot be determined in either case. We can estimate an upper bound for  $\Delta\bar{\mu}$  for the <sup>1</sup>L<sub>b</sub> transition, which is 2.0 D in both protonation states and is likely considerably less. For the <sup>1</sup>L<sub>a</sub> transition in both the protonated and deprotonated states, there are small but non-negligible contributions to the Stark spectra from the zeroth and first derivative terms. The contribution from the positive zeroth derivative suggests that the values of the transition polarizability, **A**, and the transition hyperpolarizability, **B**, are small but nonzero. The precise contributions from each of these terms cannot be determined from the experimental data in this study. The positive first derivative component shows that the change in polarizability,  $\Delta\alpha$ , is only 6 Å<sup>3</sup> for the protonated state and 3 Å<sup>3</sup> for the deprotonated state.

It should be noted that temperature and matrix effects can also have an influence on charge reorganization in the excited state. Excited-state proton transfer was not observed for HPTS in a glassy water/glycerol mixture at 77 K. From comparing the fluorescence spectra of HPTS in glycerol<sup>32</sup> and water,<sup>35</sup> the solvent environment of the water/glycerol mixture is very similar to aqueous conditions at room temperature. The low temperature absorption spectrum of the water/glycerol mixture differs somewhat from the room temperature spectrum. However, the temperature effects on the Stark spectra in previous studies of

similar photoacid-like molecules have shown a very small temperature dependence.<sup>36</sup>

These results indicate that for both the protonated and deprotonated states, there is a moderate amount of charge redistribution upon excitation, and such redistribution is dominated by a change in dipole moment upon excitation, rather than a large change in polarizability. The difference between the values of  $\Delta\bar{\mu}$  for the two protonation states is small ( $\sim 1$  D), and this difference can be accounted for by the fact that there is simply more charge available to redistribute in the deprotonated form. This is in contrast to previous computational studies suggesting that charge transfer in the lowest excited state occurs almost exclusively for the deprotonated species. Furthermore, this is consistent with the idea that there is a significant charge redistribution immediately upon excitation of the protonated species and before deprotonation occurs.

Evidence specifically for the movement of charge from the hydroxyl oxygen into the aromatic system in the protonated state is provided by the angle dependence of the Stark spectrum. The angle  $\zeta_A$  between the difference dipole moment and the transition dipole moment of the protonated form of HPTS was measured to be 30°, and this angle is approximately the same for all molecules studied here. The value of 30° is in agreement with the angle between the electron donor (hydroxyl group) and the <sup>1</sup>L<sub>a</sub> transition dipole direction along the long axis of the molecule (see Figure 1), which has been previously measured.<sup>32,37</sup> This angle is consistent with the notion that the change in dipole upon excitation is due to migration of charge density from the hydroxyl oxygen into the aromatic system. The Stark spectrum provides the magnitude of  $\Delta\bar{\mu}$  (eq 6), not its sign. Because both proposed mechanisms for photoacidity predict a movement of charge density from the acidic group into the aromatic ring, it is reasonable to assume that the direction of  $\Delta\bar{\mu}$  is from the acidic group toward the aromatic ring, rather than the opposite direction, in all cases studied here.

**B. 1-Pyrenol (PyOH).** The case of pyrenol (PyOH) is more complicated because the lowest electronic states invert during the excited-state proton-transfer process. The absorption and Stark spectra of the protonated and deprotonated states are shown in Figure 4. The lowest energy band for the protonated state corresponds to the <sup>1</sup>L<sub>b</sub> transition, but the <sup>1</sup>L<sub>a</sub> transition is the lowest energy band in the deprotonated state.<sup>32,38</sup> Therefore, there is a <sup>1</sup>L<sub>b</sub>–<sup>1</sup>L<sub>a</sub> electronic state inversion during the excited-state proton-transfer reaction. This type of <sup>1</sup>L<sub>b</sub>–<sup>1</sup>L<sub>a</sub> electronic state inversion has been observed previously in other photoacids. For example, experiments and calculations on 1-naphthol show that within 4.5 ps of excitation to the <sup>1</sup>L<sub>b</sub> state (S<sub>0</sub> to S<sub>1</sub>), vibronic coupling between the naphthol and the solvent causes inversion of the <sup>1</sup>L<sub>b</sub> state to the more polar <sup>1</sup>L<sub>a</sub> state.<sup>39</sup> Both the <sup>1</sup>L<sub>a</sub> and <sup>1</sup>L<sub>b</sub> absorption bands contribute to the Stark spectrum of PyOH in the protonated state, with a value of  $\Delta\bar{\mu}$  of 0.9 D for the <sup>1</sup>L<sub>b</sub> transition and 2.0 D for the <sup>1</sup>L<sub>a</sub> transition. There is a significant

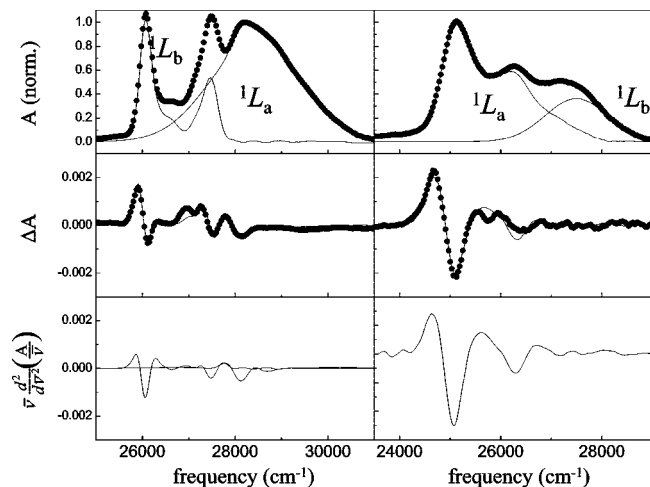


**Figure 4.** Absorption and Stark spectra of protonated (left) and deprotonated (right) PyOH. Top panels: absorption spectra (circles) and deconvolution of the spectra into  ${}^1L_a$  and  ${}^1L_b$  (solid lines) components. Middle panels: Stark spectra (circles) and fits of the Stark spectra to a sum of zeroth, first, and second derivatives of the absorption spectra (lines). Bottom panels: second derivative components of the fits to the  ${}^1L_a$  (solid lines) and  ${}^1L_b$  (dashed line) bands. The second derivative of the  ${}^1L_b$  band for the deprotonated state is not included because it does not contribute to the Stark spectrum.

contribution of the first derivative component to the Stark spectrum of the  ${}^1L_b$  transition, as can be seen in the left-middle panel of Figure 4. This is not due to an especially large change in polarizability upon excitation ( $\Delta\alpha = 5 \text{ \AA}^3$ ). Rather, because  $\Delta\bar{\mu}$  is so small, the second derivative component makes a relatively smaller contribution to the Stark spectrum than in other compounds, which makes the first derivative component more visible. The sharpness of the peaks in the  ${}^1L_b$  spectrum results in large features in the Stark spectrum even though the parameters resulting from the fit are relatively small. It is also observed that spurious first derivative-like features can arise from pure second derivative Stark effects of overlapping bands because  $\Delta A$  can be positive or negative, which can overestimate the first derivative component of the Stark spectrum. In the deprotonated state, the Stark spectrum is dominated by the second derivative of the  ${}^1L_a$  transition, and it has a value of  $\Delta\bar{\mu}$  of 2.9 D and a value of  $\Delta\alpha$  of  $5 \text{ \AA}^3$ . It is again not possible to assign  $\Delta\bar{\mu}$  precisely for the  ${}^1L_b$  transition because, as discussed above, the effect is so small. The upper bound is 2.5 D.

Similar to the observation for HPTS, the electron redistribution is much greater in PyOH for the  ${}^1L_a$  than the  ${}^1L_b$  transition, with  $\Delta\bar{\mu}$  being larger by more than a factor of 2 in the protonated state. The difference in charge transfer between the  ${}^1L_a$  and  ${}^1L_b$  transitions is even greater for the deprotonated species. As was the case for HPTS, the values of  $\Delta\bar{\mu}$  between the protonated and deprotonated states of PyOH are similar for the same electronic transition, again within  $\sim 1$  D. Although the values of  $\Delta\bar{\mu}$  for the  ${}^1L_b$  transition are small for both HPTS and PyOH, the values of  $\Delta\bar{\mu}$  for the  ${}^1L_a$  transition are notably smaller for PyOH than for HPTS. This is likely due to the fact that PyOH lacks the three electronegative sulfonate groups that are present on the aromatic ring of HPTS, thereby making the aromatic ring of PyOH a poorer electron acceptor as charge from the hydroxyl oxygen is donated into the  $\pi$  system.

**C. 8-Aminopyrene-1,3,6-trisulfonate (APTS).** 8-Aminopyrene-1,3,6-trisulfonate (APTS) is fundamentally different from the other photoacids examined herein in that it has an amine moiety as the acidic group instead of a hydroxyl. Therefore, in the protonated state, it has no free electrons on the acidic group

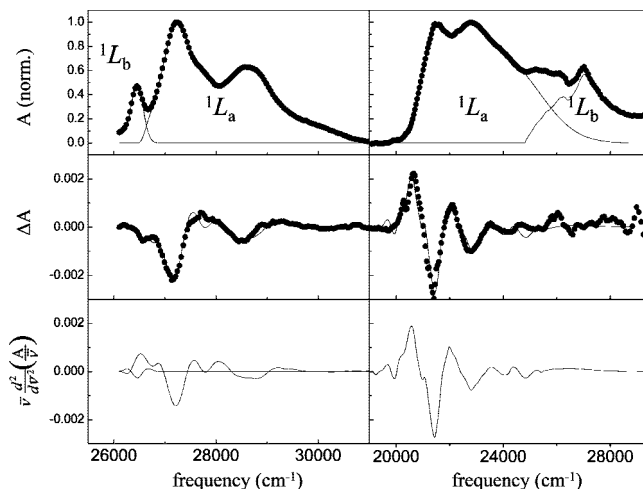


**Figure 5.** Absorption and Stark spectra of protonated (left) and deprotonated (right) APTS. Top panels: absorption spectra (circles) and deconvolution of the spectra into  ${}^1L_a$  and  ${}^1L_b$  (solid lines) components. Middle panels: Stark spectra (circles) and fits of the Stark spectra to a sum of zeroth, first, and second derivatives of the absorption spectra (lines). Bottom panels: second derivative components of the fits to the  ${}^1L_a$  (solid lines) and  ${}^1L_b$  (dashed line) bands.

to donate into the aromatic ring. Despite this, the shift in  $pK_a$  of APTS upon photoexcitation is estimated to be 10 units. Thus, APTS should provide a good test of the idea that charge rearrangement in the protonated state is necessary for photoacidity.

The state ordering of APTS is similar to that of PyOH, in that the  ${}^1L_b$  transition is lower in energy in the protonated state, whereas the  ${}^1L_a$  transition is lower in energy in the deprotonated state. As shown in Figure 5, both the  ${}^1L_a$  and  ${}^1L_b$  lineshapes contribute to the Stark spectrum in the protonated state. The value of  $\Delta\bar{\mu}$  in the  ${}^1L_b$  transition (0.6 D) is much smaller than in the  ${}^1L_a$  transition (2.2 D). In the deprotonated state (Figure 5), the Stark spectrum is dominated by the  ${}^1L_a$  transition, which has a relatively large value of  $\Delta\bar{\mu}$  (5.3 D). Again, the values of  $\Delta\alpha$  are small for all transitions. For the  ${}^1L_a$  transition in the protonated state,  $\Delta\alpha$  is negative, which is in contrast to the other cases in this study. This is likely due to the presence of a positive charge and no free electrons on the acidic group, whereas the acidic group is neutral or negatively charged and contains at least one free pair of electrons that can be redistributed into the aromatic system in all other cases. Again no Stark effect was observed for the  ${}^1L_b$  transition in the deprotonated state, and  $\Delta\bar{\mu}$  for this transition is less than 2.1 D. As stated earlier, this is an upper bound for the measurement and the actual value is most likely significantly smaller.

As expected for an amine photoacid, the charge redistribution in the protonated state is small for both the  ${}^1L_a$  and  ${}^1L_b$  transitions, presumably due to the lack of a nonbonding electron pair on the acidic moiety. Despite the relatively small amount of charge redistribution in the protonated state upon photoexcitation, APTS is a very strong photoacid with a large shift in  $pK_a$  upon excitation. This suggests that substantial charge redistribution in the protonated state directly upon excitation is not required in all cases for photoacidity to occur. In the deprotonated state, which has a nonbonding pair of electrons on the amine nitrogen, the charge redistribution is much larger than in the protonated state. Therefore, APTS conforms to the scenario in which charge redistribution occurs primarily after proton dissociation.

The deprotonated form of APTS is interesting in that it is isoelectronic with HPTS, thus allowing a direct comparison of

these two species with respect to their charge redistribution. By comparing the Hammett parameters for  $-\text{NH}_2$  and  $\text{O}^-$  ( $\sigma_p = -0.66$  and  $-0.81$ , respectively),<sup>40</sup> it is expected that the electronic properties of the deprotonated forms of APTS and HPTS should be very similar. Both the steady-state and transient absorption electronic spectra for the two molecules have been shown to agree very well.<sup>41</sup> The Stark spectra of the two molecules are also nearly identical. Given these similarities, it is not surprising that the electron redistribution in deprotonated APTS is similar to the large redistribution found for HPTS.

#### IV. Conclusions

The results presented herein demonstrate that there is no single mechanism responsible for the shift in  $\text{p}K_a$  in all photoacids. Even among the structurally similar group of pyrene photoacids examined, there is considerable variation in the amount of charge redistribution as a function of protonation state. The results for HPTS are consistent with the scenario in which charge redistribution occurs directly upon photoexcitation, followed by proton dissociation, such that the photoacidity is due to an increase in the acidity of the protonated state. Conversely, results for the electronically similar APTS are consistent with the opposite scenario, in which deprotonation occurs first, followed by charge rearrangement, thereby implying that the photoacidity is due to a decrease in the basicity of the deprotonated state. From the Stark data alone, it is impossible to rule out the possibility that the protonated form of APTS undergoes a charge rearrangement at some time after photoexcitation but before proton dissociation. However, a recent time-resolved study of APTS showed that no further charge-transfer processes occurs after photoexcitation,<sup>35</sup> indicating that the total amount of charge redistribution is a mere 0.6 D preceding proton transfer.

From the Stark spectra, it appears that the amount of charge transfer depends more upon the electronic state that is excited than on the protonation state. PyOH and APTS, both of which have a  ${}^1\text{L}_b$ – ${}^1\text{L}_a$  state inversion, have much more charge redistribution for the  $\text{S}_0$  to  $\text{S}_1$  transition in the deprotonated state than in the protonated state. This is consistent with gas-phase calculations of charge transfer in phenol, which also has a  ${}^1\text{L}_b$ – ${}^1\text{L}_a$  state inversion. The calculations indicate that charge redistribution occurs primarily in the deprotonated state; however, it is noted that solvent effects may also be important for these systems. HPTS, which does not have a state inversion, has significant charge redistribution in both protonation states. Although further studies are needed to confirm these trends for a wider variety of photoacids, this work suggests that in other photoacids that have a  ${}^1\text{L}_b$ – ${}^1\text{L}_a$  state inversion, such as phenols or 1-naphthols, the deprotonated state can be expected to undergo more charge rearrangement than the protonated state. However, photoacids that do not have a state inversion, such as 2-naphthols and the chromophore in GFP,<sup>20</sup> should have similar charge-transfer characteristics in the protonated and deprotonated states.

**Acknowledgment.** This work was supported by the Department of Energy (DE-FG03-84ER13251) and National Institute

of Health (GM027738). N.L.S. thanks the National Science Foundation for an NSF Fellowship.

#### References and Notes

- (1) Weller, A. Z. *Phys. Chem.* **1958**, *17*, 224.
- (2) Elsaesser, T.; Bakker, H. J. *Ultrafast Hydrogen Bonding Dynamics and Proton Transfer Processes in the Condensed Phase*; Kluwer Academic Publishers: Dordrecht, The Netherlands, 2002.
- (3) Pines, E. In *The Chemistry of Phenols*; Rappoport, Z., Ed.; John Wiley & Sons: West Sussex, U.K., 2003; Vol. 1, pp 491.
- (4) Glodde, M.; Goldfarb, D. L.; Medeiros, D. R.; Wallraff, G. M.; Denbeaux, G. P. *J. Vac. Sci. Technol. B* **2007**, *25*, 2496.
- (5) Wang, M.; Wang, Y.; Gonsalves, K. E. *Macromolecules* **2007**, *40*, 8220.
- (6) Kim, K.-M.; Ayothi, R.; Ober, C. K. *Polym. Bull.* **2005**, *55*, 333.
- (7) Tolbert, L. M.; Haubrich, J. E. *J. Am. Chem. Soc.* **1990**, *112*, 8163.
- (8) Cheshnovsky, O.; Leutwyler, S. *J. Chem. Phys.* **1988**, *88*, 4127.
- (9) Knochenmuss, R.; Cheshnovsky, O.; Leutwyler, S. *Chem. Phys. Lett.* **1988**, *144*, 317.
- (10) Knochenmuss, R.; Muino, P. L.; Wickleder, C. *J. Phys. Chem.* **1996**, *100*, 11218.
- (11) Knochenmuss, R.; Karbach, V.; Wickleder, C.; Graf, S.; Leutwyler, S. *J. Phys. Chem. A* **1998**, *102*, 1935.
- (12) Solntsev, K. M.; Huppert, D.; Agmon, N. *J. Phys. Chem. A* **1999**, *103*, 6984.
- (13) Solntsev, K. M.; Huppert, D.; Tolbert, L. M.; Agmon, N. *J. Am. Chem. Soc.* **1998**, *120*, 7981.
- (14) Pines, E.; Huppert, D. *Chem. Phys. Lett.* **1986**, *126*, 88.
- (15) Pines, E.; Huppert, D. *J. Chem. Phys.* **1986**, *84*, 3576.
- (16) Förster, T.; Volker, S. *Chem. Phys. Lett.* **1975**, *34*, 1.
- (17) Mohammed, O. F.; Pines, D.; Dreyer, J.; Pines, E.; Nibbering, E. T. *J. Science* **2005**, *310*, 83.
- (18) Lewis, F. D.; Sinks, L. E.; Weigel, W.; Sajimon, M. C.; Crompton, E. M. *J. Phys. Chem. A* **2005**, *109*, 2443.
- (19) Zhou, W.; Kuebler, S. M.; Carrig, D.; Perry, J. W.; Marder, S. R. *J. Am. Chem. Soc.* **2001**, *124*, 1897.
- (20) Chattoraj, M.; King, B. A.; Bublitz, G. U.; Boxer, S. G. *Proc. Natl. Acad. Sci. U.S.A.* **1996**, *93*, 8362.
- (21) Leiderman, P.; Ben-Ziv, M.; Genosar, L.; Huppert, D.; Solntsev, K. M.; Tolbert, L. M. *J. Phys. Chem. B* **2004**, *108*, 8043.
- (22) Rappoport, Z. *The Chemistry of Phenols*; Wiley: New York, 2003.
- (23) Hynes, J. T.; Tran-Thi, T.-H.; Granucci, G. *J. Photochem. Photobiol. A Chem.* **2002**, *154*, 3.
- (24) Jeffrey, G. A. *J. Mol. Struct.* **1994**, *322*, 21.
- (25) Tran-Thi, T. H.; Prayer, C.; Millie, P.; Uznanski, P.; Hynes, J. T. *J. Phys. Chem. A* **2002**, *106*, 2244.
- (26) Granucci, G.; Hynes, J. T.; Millie, P.; Tran-Thi, T.-H. *J. Am. Chem. Soc.* **2000**, *122*, 12243.
- (27) Agmon, N.; Retting, W.; Groth, C. *J. Am. Chem. Soc.* **2002**, *124*, 1089.
- (28) Weller, A. *Electrochemistry* **1952**, *56*, 662.
- (29) Ireland, J. F.; Wyatt, P. A. H. *Adv. Phys. Org. Chem.* **1976**, *12*.
- (30) Agmon, N. *J. Chem. Phys.* **1987**, *88*, 5639.
- (31) Andrews, S. S.; Boxer, S. G. *Rev. Sci. Instrum.* **2000**, *71*, 3567.
- (32) Spry, D. B.; Goun, A.; Fayer, M. D. *J. Chem. Phys.* **2006**, *125*, 144514.
- (33) Platt, J. R. *J. Chem. Phys.* **1949**, *17*, 484.
- (34) Chowdhury, A.; Locknar, S. A.; Premvardhan, L. L.; Peteanu, L. A. *J. Phys. Chem. A* **1999**, *103*, 9614.
- (35) Spry, D. B.; Fayer, M. D. *J. Chem. Phys.* **2008**, *128*, 084508.
- (36) Premvardhan, L. L.; Peteanu, L. A. *J. Phys. Chem. A* **1999**, *103*, 7506.
- (37) van Gurp, M.; van Heijnsbergen, T.; van Ginkel, G.; Levine, Y. K. *J. Chem. Phys.* **1988**, *90*, 4103.
- (38) Michl, J. *J. Am. Chem. Soc.* **1978**, *100*, 6872.
- (39) Knochenmuss, R.; Fischer, I.; Luhrs, D.; Lin, Q. *Isr. J. Chem.* **1999**, *39*, 221.
- (40) Hansch, C.; Leo, A.; Taft, R. W. *Chem. Rev.* **1991**, *91*, 165.
- (41) Spry, D. B.; Fayer, M. D. *J. Chem. Phys.* **2007**, *127*, 204501.